Anhysteretic remanent magnetization: model of grain size distribution of spherical magnetite grains

CARLOS A. VASQUEZ[1,2], FACUNDO F. SAPIENZA[3], AGUSTÍN SOMACAL[3] AND SABRINA Y. FAZZITO[2]

1 Universidad de Buenos Aires, Ciclo Básico Común, Ramos Mejía 841, Ciudad Autónoma de Buenos Aires, Argentina

2 CONICET, IGEBA, Fac. Cs. Exactas y Naturales, Dto. Geología, Pab. 2, Ciudad Universitaria, Ciudad Autónoma de Buenos Aires, Argentina (vasquez@gl.fcen.uba.ar)

3 Universidad de Buenos Aires, FCEN, Dto. de Física, Pab. 1, Ciudad Universitaria, Ciudad Autónoma de Buenos Aires, Argentina

Received: April 24, 2017; Revised: September 25, 2017; Accepted: December 12, 2017

ABSTRACT

A phenomenological model based on a linear relationship between the magnetic coercivity field and the reciprocal of the grain diameter is applied to explain the anhysteretic remanent magnetization (ARM) imparted to artificial samples with different concentrations of a very well characterized magnetite powder. By analyses of scanning electron microscopy images, the spherically shaped single domain synthetic magnetite is found to follow a lognormal grain size distribution with ~86 nm of mean diameter. The proposed model, fitted to ARM measurements up to a peak alternating field of 100 mT, yields a very good agreement. The coercivity behaviour predicted by micromagnetism theory disagrees with the experimental results of this work. A likely explanation for the discrepancy is that the magnetite particles, which consist of a mixture of grains in coherent rotation and curling modes, produce similar observations as domain processes.

Keywords: micromagnetism, magnetite, ARM, SEM, thermomagnetic curves

1. INTRODUCTION

1.1. Anhysteretic remanent magnetization and grain size distribution

Anhysteretic remanent magnetization (ARM) and alternating field degaussing (AF) have been extendedly used in several rock magnetism applications: identification of magnetic minerals (e.g., *Nagata, 1961*; *Dunlop and Özdemir, 1997*), isolation of magnetic vectors in palaeomagnetism (e.g., *Butler, 1992; Tauxe et al., 2016*) and anisotropy of anhysteretic remanent magnetization (AARM; e.g., *McCabe et al., 1985*; *Jackson et al., 1989*; *Jackson, 1990, 1991*). The first pioneering work on ARM was made by *Maurain (1904)*, but the first investigation of ARM in rocks and minerals, according to *Nagata*

(1961), were developed by Thellier, Rimbert and Petrova (*Thellier and Rimbert, 1954, 1955*; *Petrova, 1957, 1959*).

ARM and AF are closely related because a decreasing alternating magnetic field is involved in both methods. In the ARM procedures, an alternating magnetic field is superimposed on a constant magnetic field H_{DC}, so that the total field $H(t)$ is given by:

$$H(t) = H_{AF}(t)\sin(\omega t) + H_{DC}, \tag{1}$$

where t is the time, ω the angular frequency and $H_{AF}(t)$ the amplitude of the AF field.

Schmidbauer and Schembera (1987) found a strong dependence of ARM on grain size in artificial samples of magnetite with average grain diameters of 61, 85, 127 and 162 nm. *Liu et al. (2005b)* modeled the grain size distribution (GSD) of magnetite grains in Chinese loess in the superparamagnetic (SP)/single domain (SD) threshold, near 25–30 nm. This model is based on the temperature and frequency dependence of the initial magnetic susceptibility.

1.2. Micromagnetism and grain size distribution

The relationships between magnetic properties and grain size of ferromagnetic grains have been discussed from the early Néel's papers (*Néel, 1932, 1948, 1950, 1951*; *Smart, 1955*) in the context of the Stoner-Wohlfarth domains theory (*Stoner and Wohlfarth, 1948*; *Tannous and Gieraltowski, 2008*). Micromagnetic theory (*Brown, 1963*) provided new insights from first principles and, for the first time, non-coherent rotation modes of magnetization were proposed. *Muxworthy et al. (2003)* found that vortex, fanning or diagonal magnetization modes were possible and calculated that the critical size between coherent and non-coherent rotation for magnetite was near 70 nm in diameter. By using micromagnetic calculations, they encountered that beyond this critical size, the magnetic properties vary significantly (see also *Muxworthy and Williams, 2006*). *Tauxe (2002)* proposed a flower mode, which is intermediate between the coherent and the vortex configuration for grains near 70 nm, while the vortex rotation mode was calculated for grains of about 100 nm. If the grain size distribution is mostly centered at 70 nm and the tail towards the larger grain sizes is long, the magnetic properties seem to be driven by non-coherent mode. It is worthwhile to mention that these modes occur only during the magnetization process. After this, the magnetization is uniform, but the magnitude is dependent of the acquisition mode (*Dunlop and West, 1969*). On the other hand, *Bertotti (1998)* proposed, for systems made of fine particles, four dominant grain size-dependent magnetization mechanisms. These are, starting from the smaller diameters: thermal relaxation (superparamagnetism), coherent rotation (Stoner-Wohlfarth model), curling (flower and vortex mode) and domain processes (multidomain). Their coercivity varies with the grain size as it is shown in Fig. 1 (*Bertotti, 1998*).

Though *Egli and Lowrie (2002)* proposed a deeply founded theory of ARM in good accordance with the experimental results of the CS914 sample from the Yucca Mountain Tuff, which was first studied by *Eick and Schlinger (1990)* and *Worm and Jackson (1999)*, the grain size distribution parameters from Electron Microscopy (Scanning or Transmission) was not showed in any of these papers. The magnetic behavior of the particles of the CS914 sample (prolate grains with a medium size of 8.5×45 nm) varies

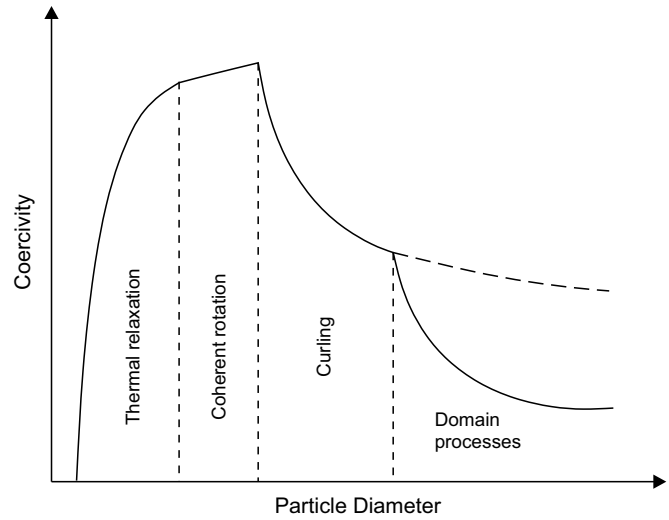

Fig. 1. Schematic sketch of magnetic coercivity versus grain size diameter. Modified from *Bertotti (1998)*.

between coherent rotation and curling (vortex) modes. According to *Bertotti (1998)*, the magnetization mechanism is very complex and phenomenological models are preferred.

In order to achieve a better understanding of the magnetization acquisition process, an ARM was applied to several artificial samples of BAYFERROX 318 BR (Bayer Co.) magnetite in a diamagnetic epoxy matrix to prevent magnetic interactions with concentrations of ~0.1 and 1.0% (weight). The grain size distribution is very well characterized first by studying Scanning Electron Microscope (SEM) images of bulk magnetite powder. A simple model is proposed, based on phenomenological theory that relates the ARM magnetization with the grain size distribution of spherical particles of magnetite. The reliability of the model is evaluated by curve fitting of experimental data and by comparing the resulting parameters with those determined from the SEM analysis.

2. THEORETICAL MODEL

In this work, we propose a phenomenological model for the ARM magnetization of spherical magnetite grains which is founded in a cause-effect relationship. The peak alternating magnetic field H_{AF}^{max}, the direct magnetic field H_{DC}, the grain size diameter d and the magnetic coercivity H_c of the grains are involved among the causes, while the effect is given by the intensity of magnetization M^{tot} acquired by the sample. Magnetization mechanisms are not considered in this simple approach as a way to avoid the complex and, sometimes, controversial world of micromagnetics (e.g., *Aharoni, 2001*).

The coercivity H_c is supposed to be dependent of the grain diameter *d* according to:

$$H_c(d) = Ad^{-\alpha} + B, \tag{2}$$

where *A*, α, and *B* are constants to be determined. In the model we assume that $\alpha = 1$. As we will discuss in Section 4.4, this hypothesis, at the same time, provides the best fitting of ARM data and corresponds to a known physical process proposed by *Bertotti (1998)* in the field of micromagnetics.

The ARM is supposed to be dependent of the grain volume, according to the following equation:

$$M(d) = K_0 d^{3\beta}, \tag{3}$$

where K_0 is a positive constant. We assume for simplicity that $\beta = 1$.

Then, the total ARM, with peak field H_{AF}^{max}, acquired by an ensemble of grains with a grain size distribution $f_d(s)$, where *s* is the integration variable and $H_c(s)$ the magnetic coercivity such that $H_c(s) \le H_{AF}^{max}$ is, using a reasoning similar to *Chantrell et al. (1977)*:

$$M^{tot}\left(H_{AF}^{max}\right) = \int_{\left\{d: H_c(d) \le H_{AF}^{max}\right\}} M(s) f_d(s)\, ds. \tag{4}$$

O'Grady and Bradbury (1983), among others, studied the effects of the grain size distribution of synthetic ferrofluids (SP particles) on magnetic properties. They found that the grain size distribution can be described by a lognormal probability function. Moreover, if the diameters are lognormally distributed, the volume follows then a lognormal distribution too (*O'Grady and Bradbury, 1983*). The magnetite used in this work is synthetic, so it seems plausible to propose a lognormal distribution $f_d(s)$ for the spherical grain diameters, which is in agreement with the chemical origin of these particles (*Vasquez et al., 2009*):

$$f_d(t) = \frac{1}{\sqrt{2\pi}\sigma t} \exp\left[-\frac{(\ln t - \mu)^2}{2\sigma^2}\right], \tag{5}$$

where *t* is the variable (diameter) and μ (mean particle diameter) and σ (standard deviation) are the two parameters of the distribution.

The solution of Eq. (4) is therefore:

$$M^{tot}\left(H_{AF}^{max}\right) = C\left[1 + \operatorname{erf}\left(D \ln\left(H_{AF}^{max} - E\right) + F\right)\right], \tag{6}$$

where $\operatorname{erf}(\cdot)$ is the error function, and *C*, *D*, *E* and *F* are constants to be determined. The standard deviation σ can be related to *D* according to the following equation:

$$D = \frac{1}{\sqrt{2}\sigma\alpha}. \tag{7}$$

The parameters obtained from fitting the model to experimental data can be used to know the standard deviation σ of the grain size distribution. Though a proper description of this distribution is given by both the standard deviation σ and the mean μ, the later is unknown from the model. However, the quotient between σ and μ, which it is known as the coefficient of variation θ, is given by:

$$\theta = \sqrt{\exp\left(\sigma^2\right) - 1}. \tag{8}$$

This coefficient, which is a function of σ and can be calculated from experimental results, provides information about the grain size distribution.

3. EXPERIMENTS

Three samples containing BAYFERROX 318 BR (Bayer Co.) spherically shaped synthetic magnetite powder were prepared in an ARALDITE diamagnetic epoxy resin matrix to avoid magnetic interactions (Table 1): two twin-samples with concentrations near 1.0% (weight) and one sample with a concentration of about 0.1% (weight).

Stepwise acquisition of ARM magnetization in peak alternating fields up to 100 mT was applied to the three samples, with a coaxial steady field of 200 μT for sample 1A and with a direct field of 300 μT for samples 1B and 2A. An AGICO LDA-3A AF demagnetizer/AMU-1A anhysteretic magnetizer was used to impart the artificial magnetization which was measured with an AGICO JR6 spinner magnetometer at each step.

Variation of magnetic susceptibility with temperature of a small amount of magnetite powder was determined with an AGICO MFK1-FA Multi-Function Kappabridge coupled to high-temperature (CS4) and low-temperature (CSL) controllers, from −180 to 700°C (976 Hz, 200 Am^{-1}), in order to establish its purity and detect oxidation processes. A 5-mm-diameter quartz glass test tube was used as sample holder. Liquid nitrogen

Table 1. Concentration and properties of the three samples prepared in a diamagnetic epoxy resin (Araldite) cement matrix. The mean diameter of the magnetite grains, obtained from SEM images, is ~86 nm.

Sample	Concentration [weight %]	Properties
1A and 1B	1.37	Bayferrox (Bayer Company) synthetic iron oxide (Fe_3O_4) powder in diamagnetic matrix. Spherically shaped single domain magnetite. Mean diameter ~86 nm.
2A	0.19	

(~ 77 K) was applied to reach low temperatures. High-temperature susceptibility measurements were done under argon atmosphere to prevent oxidation.

SEM images were analysed with the aim of validating the hypothesis of lognormal grain size distribution in a bulk sample of magnetite powder. Several microphotographies with low and high magnification (with scale bars of 100, 200, 300 and 1000 nm) were obtained by means of a Zeiss SUPRA-40 SEM at Centro de Microscopías Avanzadas (Fac. Cs. Exactas y Naturales, Universidad de Buenos Aires). Grain size distribution was estimated with the help of the ImageJ open source image processing software. Magnetite grains were highlighted in the SEM images as ellipses but, due to clustering, algorithms failed to recognize their shapes and then automatic counting was not possible. Finally, the number of particles was determined by visual inspection of three 300-nm scale SEM images. A mean diameter for each grain was calculated from the area of the ellipses. A total of 964 grains were detected from these microphotographies. This process was done by two operators working in different days to avoid statistical biasing. Both obtained similar results.

4. RESULTS AND DISCUSSION

4.1. Acquisition of ARM

Regardless of the bias magnetic field, a similar behaviour in the acquisition of normalized ARM is observed for the three artificial specimens, which reach saturation for alternating fields greater than ~70–80 mT (Fig. 2). In particular, no significant difference is noticed for the twin samples 1A and 1B, which were subjected to a direct field of 200 μT and 300 μT, respectively.

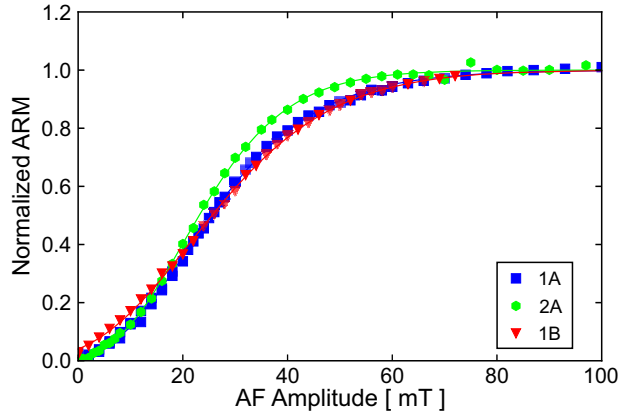

Fig. 2. Normalized acquisition of anhysteretic remanent magnetization (ARM) in a DC field of 200 μT for sample 1A, and in a DC field of 300 μT for samples 1B and 2A. The solid curves represent results of theoretical fitting the experimental data (symbols).

4.2. Variation of magnetic susceptibility with temperature

The thermomagnetic curve determined from a bulk sample of BAYFERROX magnetite powder (Fig. 3) shows that, in the low-temperature region, the Verwey transition is suppressed. For isolated spherical grains, the crystalline anisotropy prevails over the shape anisotropy and the Verwey transition is expected. However, considering that the dependence of magnetic susceptibility with temperature was measured on a small amount of magnetite powder contained in a cylindrical-shaped holder, the most important contribution is, on the contrary, given by the shape anisotropy and thus the Verwey transition is absent. In the high-temperature zone, the Hopkinson peak and the Curie temperature both near 580°C agree with the presence of stable single domain (SSD) magnetite. On the other hand, *Worm (1998)* showed that the increase of magnetic susceptibility from low to high temperatures could be attributed to a lognormal distribution of grains in the SSD/SP limit. The blocking temperature is dependent of frequency and temperature. At a fixed frequency, the increasing in temperature causes the SSD fraction to go to SP fraction in the SSD/SP limit. Figure 3 shows that the magnetic susceptibility increases and decreases monotonously due to the SP fraction, which is unblocked during the heating and blocked in the cooling process (*Liu et al., 2005a*). An alternative explanation could be an oxidation process that produces maghemitization of magnetite (*Dunlop and Özdemir, 1997*), but heating and cooling curves are in agreement with a partial oxidation of magnetite to maghemite that after heating is oxidized to hematite and so the susceptibility is lower for the cooling curve (*Gehring et al., 2009*).

4.3. SEM images and grain size distribution

The empirical grain size distribution obtained from the SEM microphotographies (representative images are shown in Fig. 4) were smoothed by a Gaussian kernel density

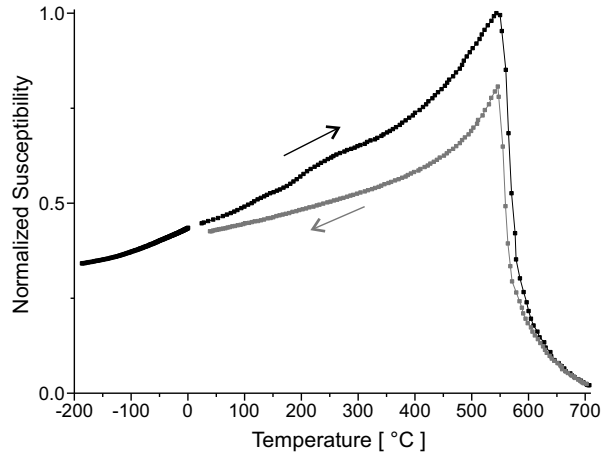

Fig. 3. Variation of normalized magnetic susceptibility with temperature for bulk magnetite powder, from –180 to 700°C. Heating and cooling curves are indicated by arrows. The Hopkinson peak and the Curie temperature are in agreement with stable single domain magnetite; the reason for the Verwey suppression (near –150°C) is explained in the text.

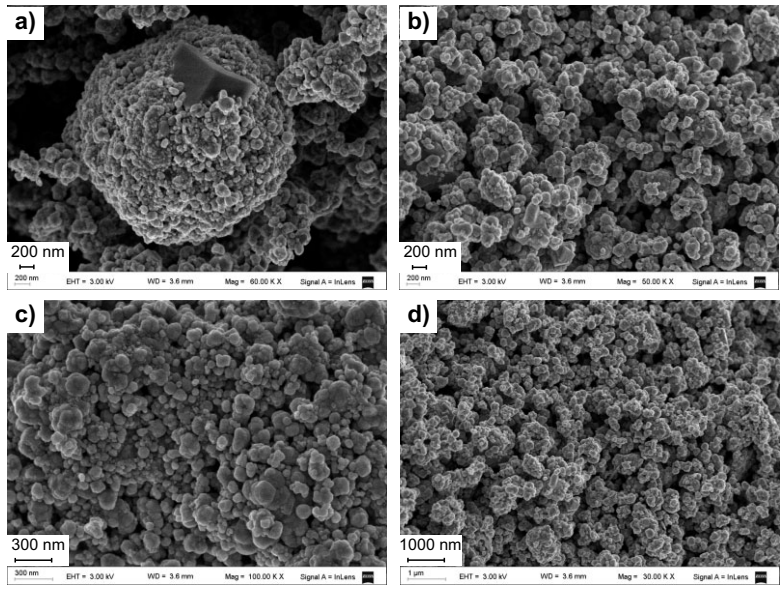

Fig. 4. SEM images with three different scale bars: **a)** and **b)** 200 nm (see that magnetite cubes are recognizable); **c)** 300 nm (image that was used to determine the grain size distribution); **d)** 1000 nm (microphotography that provides a panoramic view of the sample).

plot and then fitted to a lognormal distribution (Eq. (5), Fig. 5). The parameters of the distribution are 86 ± 3 nm for the mean diameter and 49 ± 2 nm for the standard deviation, with a square of correlation coefficient $R^2 = 0.995$. The coefficient of variation calculated is, according to Eq. (8), $\theta_{emp} = 0.51 \pm 0.01$. A Shapiro-Wilk hypothesis test (*Shapiro and Wilk, 1965*) shows a high level of confidence for the fitting, considering that the *p*-value is 0.22.

4.4. ARM measurements and the phenomenological model

Several studies have been carried out in order to determine the relationship between the magnetic properties and the grain size of magnetite (*McNab et al., 1968*; *Tauxe et al., 2002*; *Muxworthy et al., 2003*; *Muxworthy and Williams, 2006*). As already explained in the *Introduction* section, it has been shown, by using micromagnetism calculations, that at near 70 nm there is a change in the magnetization mode, from the coherent rotation to the curling configuration (Fig. 1). The magnetite grains used in this work follow a lognormal distribution with a mean particle diameter of ~86 nm (Fig. 5). From this distribution, it is also possible to estimate roughly that one third of these particles resides in the coherent rotation mode and that two thirds correspond to the curling mode. Considering that these comprise a mixture of rotation and curling particles, their magnetic properties can be studied to validate micromagnetism predictions. However, the phenomenological theory proposed in this work regards the coherent rotation behavior only, because all the grains are homogenously aligned in the magnetic field at the same time.

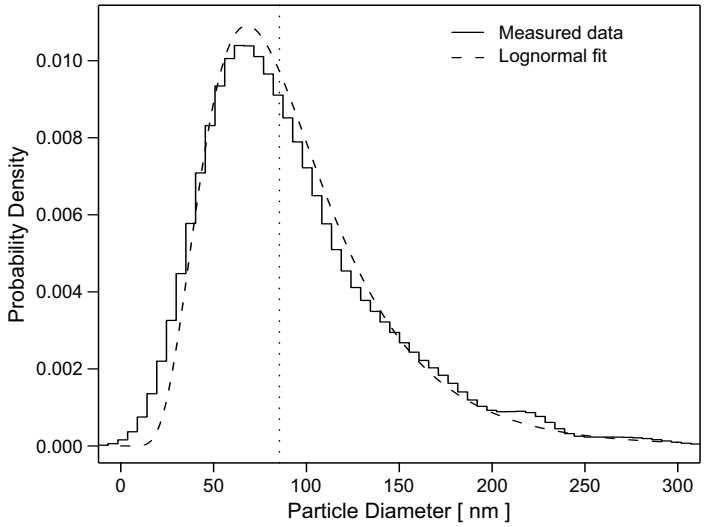

Fig. 5. Grain size distribution obtained from three SEM images with the same scale as in Fig. 4c. The results exhibit an excellent fit with a lognormal distribution with a mean particle diameter of 86 ± 3 nm (dotted line), a standard deviation of 49 ± 2 nm and a square of correlation coefficient $R^2 = 0.995$.

For each of the three curves in Fig. 2, the standard deviation σ can be calculated from the fitted parameters by using Eq. (7). Then, from Eq. (8), the associated coefficients of variation are estimated (see Table 2). A minimum value of $\theta_{ARM} = 0.25 \pm 0.03$ and a maximum value of $\theta_{ARM} = 0.34 \pm 0.03$ were determined from the proposed model. These values are in good accordance with the experimental value θ_{emp} found by direct SEM observation. The congruence of the ARM measurements and curves fitted according to Eq. (6), as suggested in Section 2, supports the hypothesis of a $1/d$ relationship between the grain diameter d and the coercivity field H_c (results from fitting experimental data are shown in Fig. 2).

At first glance, the proposed value $\alpha = 1$ in Eq. (2) could be a motive of debate. Though other values were examined during the analysis of experimental data giving also

Table 2. Standard deviations inferred from fitting procedures on measurements of anhysteretic remanent magnetization (Fig.2) and associated coefficients of variation for the three artificial samples.

Sample	Standard deviation σ [nm]	Coefficient of variation θ
1A	0.33 ± 0.02	0.34 ± 0.03
1B	0.26 ± 0.03	0.27 ± 0.02
2A	0.25 ± 0.02	0.25 ± 0.03

good results (not shown), the linear relationship between the magnetic coercivity field and the reciprocal of the grain diameter provides the best fitting and, which is most outstanding, has a direct physical interpretation. Other relation is not explained by the micromagnetic theory. This $1/d$ dependence of the coercive force on the grain size is associated to larger particles that belong to the domain processes, as suggested by *Bertotti (1998)*. The mixture of particles in the coherent and curling modes may produce similar observations as domain process.

4.5. Influence of grain size in magnetization

The contribution to the total magnetization in relation to the grain size diameter was evaluated for the synthetic magnetite powder analysed in this study. The GSD of the actual sample was used to calculate the variation of the total magnetization with the volume grain size under the hypothesis of spherical shape. The cumulative volume grain size distribution curve multiplied by the particle volume is shown in Fig. 6 and the contribution to the total magnetization of grains with size smaller than a certain diameter is indicated in Table 3.

The contribution to the magnetization of the larger grains domains over that of the smaller grains. Particles with diameters bellow 70 nm contribute only with 3.30% to the total magnetization of the sample. This grain size is usually taken by palaeomagnetists as carrying the stable remanence of magnetite. The synthetic magnetite studied in this work has a mean diameter of ~86 nm, which can be considered lower than the mean size encountered in most natural samples. It could be interpreted that, to get the "stable magnetization", it would be necessary to demagnetize until ~4% of the original magnetization, assuming that the magnetization of all the grains is saturated. However, the "net remanence" is a sum of multiple oriented magnetic vectors of magnetite grains of all grain size and PSD (pseudo-single domain) particles with vortex microstructures are also reliable/stable palaeomagnetic signal recorders (*Almeida et al.*, 2017).

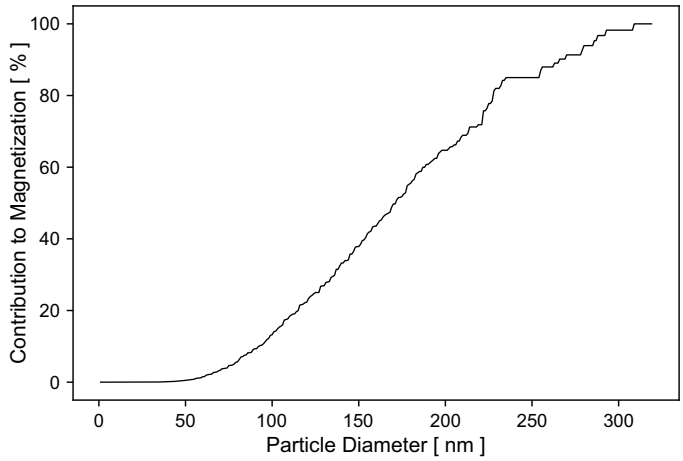

Fig. 6. Contribution to magnetization, expressed as a volume multiplied by cumulative distribution function, in dependence on the grain diameter.

Table 3. Contributions of grains with different grain sizes to the total magnetization.

Grain Size Diameter [nm]	Contribution to Total Magnetization [%]
< 70	3.30
< 80	5.65
< 90	9.34
< 100	13.25

5. CONCLUSIONS

In this work, a phenomenological model founded in a $1/d$ dependence of the magnetic coercivity on the grain diameter d was proposed to explain the ARM measurements on artificial samples with different concentrations of a very well characterized magnetite powder. Spherical grains of SD magnetite with a lognormal distribution with a mean diameter of ~86 nm were identified by a SEM microphotography study. The model was tested with ARM experimental data showing very good agreement.

The theoretical prediction of micromagnetism suggests this reciprocal dependence for larger particles residing in the domain process mode. The mixture of particles in the coherent and curling modes is probably causing similar observations. The magnetization is strongly influenced by the grain size distribution, so samples with magnetite particles with a very narrow grain size distribution could give conclusive results.

The model proposed in this work can be used to predict the magnetic behaviour in a natural sample, considering that a mixture of several ensembles of particles with different rotation modes may produce an ARM magnetization which is equivalent to domain process mode. It is an open research field.

Acknowledgements: Mr. Matias Naselli is thanked for his help in measurements. This research was financially supported by Agencia Nacional de Promoción Científica y Tecnológica (grant PICT-2014-1516). We are indebted to two anonymous reviewers for their suggestions, which improved the manuscript.

References

Aharoni A., 2001. Micromagnetics: past, present and future. *Physica B*, **306**, 1–9.

Almeida T.P., Muxworthy A.R, Kovács A., Williams W. and Dunin-Borkowski R.E., 2017. Observation of thermally-induced magnetic relaxation in a magnetic grain using off-axis electron holography. *J. Phys. Conf. Ser.*, **902**, 012001, DOI: 10.1088/1742-6596/902 /1/012001.

Bertotti G., 1998. *Hysteresis in Magnetism: For Physicists, Materials Scientists, and Engineers*. First Edition. Academic Press, San Diego, CA.

Brown W.F., Jr., 1963. *Micromagnetics*. John Wiley and Sons, Inc., New York.

Butler R.F., 1992. Paleomagnetism: Magnetic Domains to Geologic Terranes. Blackwell Scientific Publications, Boston, MA.

Chantrell R.W., Popplewell J. and Charles S.W., 1977. The effect of a particle size distribution on the coercivity and remanence of a fine particle system. *Physica B+C*, **86–88**, 1421–1422.

Dunlop D.J. and West G.F., 1969. An experimental evaluation of single domain theories. *Rev. Geophys*., **7**, 709–757.

Dunlop D.J. and Özdemir Ö., 1997. *Rock Magnetism: Fundamentals and Frontiers*. Cambridge University Press, Cambridge, U.K.

Gehring A.U., Fischer H., Louvel M., Kunze K. and Weidler P.G., 2009. High temperature stability of natural maghemite: A magnetic and spectroscopic study. *Geophys. J. Int*., **179**, 1361–1371.

Eick P.M. and Schlinger C.M., 1990. The use of magnetic susceptibility and its frequency dependence for delineation of a magnetic stratigraphy in ash-flow tuffs. *Geophys. Res. Lett.*, **17**, 783–786.

Egli R. and Lowrie W., 2002. Anhysteretic remanent magnetization of fine magnetic particles. *J. Geophys. Res.-Solid Earth*, **107**, 2209, DOI: 10.1029/2001JB000671.

Jackson M., 1990. Magnetic anisotropy of the Trenton limestone revisited. *Geophys. Res. Lett.*, **17**, 1121–1124.

Jackson M., 1991. Anisotropy of magnetic remanence: A brief review of mineralogical sources, physical origins, and geological applications, and comparison with susceptibility anisotropy. *Pure Appl. Geophys.*, **136**, 1–28.

Jackson M., Craddock J.P., Ballard M., Van der Voo R. and McCabe C., 1989. Anhysteretic remanent magnetic anisotropy and calcite strains in Devonian carbonates from the Appalachian Plateau, New York. *Tectonophysics*, **161**, 43–53.

Liu Q., Deng C., Yu Y., Torrent J., Jackson M., Banerjee S. and Zhu R., 2005a. Temperature dependence of magnetic susceptibility in an argon environment: implications for pedogenesis of Chinese loess/palaeosols. *Geophys. J. Int.*, **161**, 102–112.

Liu Q., Torrent J., Maher B.A., Yu Y., Deng C., Zhu R. and Zhao X., 2005b. Quantifying grain size distribution of pedogenic magnetic particles in Chinese loess and its significance for pedogenesis. *J. Geophys. Res.-Solid Earth*, **110**, B11102, DOI: 10.1029/2005JB003726.

Maurain C., 1904. Étude et comparaison des procédés de réduction de l'hystérésis magnétique. *J. Phys. Theor. Appl.*, **3**, 417–434 (in French).

McCabe C., Jackson M. and Ellwood B.B., 1985. Magnetic anisotropy in the Trenton limestone: results of a new technique, anisotropy of anhysteretic susceptibility. *Geophys. Res. Lett*., **12**, 333–336.

McNab T.K., Fox R.A. and Boyle A.J.F., 1968. Some magnetic properties of magnetite (Fe_3O_4) microcrystals. *J. Appl. Physics*, **39**, 5703–5711.

Muxworthy A.R., Dunlop D.J. and Williams W., 2003. High-temperature magnetic stability of small magnetite particles. *J. Geophys. Res.-Solid Earth*, **108**, 2281, DOI: 10.1029/2002JB002195.

Muxworthy A.R. and Williams W., 2006. Critical single-domain/multidomain grain sizes in noninteracting and interacting elongated magnetite particles: Implications for magnetosomes. *J. Geophys. Res.-Solid Earth*, **111**, B12S12, DOI: 10.1029/2006JB004588.

Nagata T., 1961. *Rock Magnetism*. Revised Edition. Maruzen Co. Ltd., Tokyo, Japan.

Néel L., 1932. Influence of fluctuations of the molecular field on the magnetic properties of bodies. *Ann. Phys*., **17**, 5–105.

Néel L., 1948. Proprietes magnetiques des ferrites - ferrimagnetisme et antiferromagnetisme. *Ann. Phys.*, **3**, 137–198 (in French).

Néel L., 1950. Aimantation a saturation de certains ferrites. *Comptes Rendus Hebdomadaires des Seances de L'Academie des Sciences*, **230**, 190–192.

Néel L., 1951. Effet de la dilatation thermique sur la valeur de la constante de curie des ferrites. *J. Phys. Radium*, **12**, 258–259.

O'Grady K. and Bradbury A., 1983. Particle size analysis in ferrofluids. *J. Magn. Magn. Mater.*, **39**, 91–94.

Petrova G.N., 1957. Magnitnaya stabil'nost' gornykh porod (Magnetic stability of rocks). *Izvest. Akad. Nauk SSSR Ser. Geofiz.*, **1**, 52–61 (in Russian).

Petrova G.N., 1959. On magnetic stability of rocks. *Ann. Géophys.*, **15**, 60–66.

Shapiro W.W. and Wilk M.B., 1965. An analysis of variance test for normality (complete samples). *Biometrika*, **52**, 591–611.

Schmidbauer E. and Schembera N., 1987. Magnetic hysteresis properties and anhysteretic remanent magnetization of spherical Fe_3O_4 particles in the grain size range 60-160 nm. *Phys. Earth Planet. Inter.*, **46**, 77–83.

Smart J.S., 1955. The Néel theory of ferrimagnetism. *Am. J. Phys.*, **23**, 356–370.

Stoner E.C. and Wohlfarth E.P., 1948. A mechanism of magnetic hysteresis in heterogeneous alloys. *Phil. Trans. R. Soc. Lond. A*, **240**, 599–642.

Tannous C. and Gieraltowski J., 2008. The Stoner-Wohlfarth model of ferromagnetism. *Eur. J. Phys.*, **29**, 475–487.

Tauxe L., Bertram H.N and Seberino C., 2002. Physical interpretation of hysteresis loops: Micromagnetic modeling of fine particle magnetite. *Geochem. Geophys. Geosyst.*, **3**, 1055, DOI: 10.1029/2001GC000241.

Tauxe L., Banerjee S.K., Butler R.F. and Van der Voo R, 2016. *Essentials of Paleomagnetism*. 4th Web Edition, https://earthref.org/MagIC/books/Tauxe/Essentials/.

Thellier E. and Rimbert F., 1954. Sur l'analyse d'aimantations fossiles par l''action de champs magnetiques alternatifs. *C. R. Acad. Sci. Paris*, **239**, 1399–1401 (in French).

Thellier E. and Rimbert F., 1955. Sur l'utilisation, en paleomagnétisme, de la désaimantation por champs alternatifs. *C. R. Acad. Sci. Paris*, **240**, 1404–1406 (in French).

Vasquez C.A., Orgeira M.J. and Sinito A.M., 2009. Origin of superparamagnetic particles in Argiudolls developed on loess, Buenos Aires (Argentina). *Environ. Geol*., **56**, 1653–1661.

Walton D., 1990. A theory of anhysteretic remanent magnetization of single-domain grains. *J. Magn. Magn. Mater.*, **87**, 369–374.

Worm H.-U., 1998. On the superparamagnetic-stable single domain transition for magnetite, and frequency dependence of susceptibility. *Geophys. J. Int.*, **133**, 201–206.

Worm H.-U. and Jackson M., 1999. The superparamagnetism of Yucca Mountain Tuff. *J. Geophys. Res.-Solid Earth*, **104**, 25415–25425.